

## Analysis of Multiple Failure Modes for Pile-Reinforced Slope with Soil Spatial Variability

Jing-Ze Li<sup>1</sup>, Lei-Lei Liu<sup>2</sup> and Daniel Dias<sup>3</sup>

<sup>1</sup>Key Laboratory of Metallogenic Prediction of Nonferrous Metals and Geological Environment Monitoring, Ministry of Education, School of Geosciences and Info-Physics, Central South University, Changsha 410083, P. R. China

E-mail: jingze\_li@csu.edu.cn

<sup>2</sup>Key Laboratory of Metallogenic Prediction of Nonferrous Metals and Geological Environment Monitoring, Ministry of Education, School of Geosciences and Info-Physics, Central South University, Changsha 410083, P. R. China

E-mail: csulll@foxmail.com

<sup>3</sup>Laboratory 3SR, Grenoble Alpes University, CNRS UMR 5521, Grenoble, France

E-mail: daniel.dias@univ-grenoble-alpes.fr

**Abstract:** Stabilizing piles have been widely used in slope reinforcement against landslides. Previous investigations on the stability analyses of slope stabilized with flexible piles, however, were mainly based on the deterministic methods, where the uncertainty inherent in soil properties and the pile response were rarely incorporated. This paper proposed a new integrated framework for probabilistic analysis of pile-reinforced slopes considering the interaction between piles and soils. The soil-pile interaction is modelled by the strain wedge (SW) model, and the soil spatial variability is simulated by one-dimensional random field theory. In particular, the effect of soil spatial variability on piles response and the slope failure modes are studied. Illustrative examples with parametric studies show that soil spatial variability has significant influences on the failure mode of slope and soil-pile response. The integrated framework provides an efficient solution for probabilistic analysis of pile-reinforced slope system.

Keywords: Stabilizing pile; Spatial variability; Strain wedge model; Soil-pile interaction; Slope stability.

### 1 Introduction

Stabilizing piles have been widely used to remediate post-failure slopes and to reinforce potentially unstable slopes (Gong *et al.*, 2019, Kontoe *et al.*, 2022). The stability of pile-reinforced slope can be analyzed either by uncoupled methods (e.g., plastic deformation method) or by coupled methods (e.g., strain wedge (SW) method and finite element/difference method). In uncoupled methods, the ultimate earth pressure provided by stabilizing piles is first estimated based on the plastic deformation of soil, which is then incorporated into the analysis of the factor of safety of the slope. Though the uncoupled analysis shows advantages of simplicity and efficiency, such a method ignores the flexibility of pile and soil-pile interaction, which is not in line with engineering practice. Hence, the coupled analysis that explicitly considers the soil-pile interaction dominates the stability analysis of pile-reinforced slope system.

Currently, the majority of the analyses of pile-reinforced slope is based on deterministic methods where the uncertainties in soil parameters are ignored. However, soil properties are usually exhibiting anisotropy and spatial variability due to the natural and complex process of geological formation and transformation (Jiang *et al.*, 2018). The spatial variability of soil properties has been regarded as the major uncertainty in engineering practice, but how the spatial variability affects the failure modes of pile-reinforced slope still remains an open question.

This study investigates the influence of soil spatial variability on the response of the piles and failure modes of a pile-reinforced slope. Firstly, the random field theory coupled with a multilayer technique is adopted to simulate the spatial variability of soil properties. Then, the SW method, as a theoretical solution to solve the soil-pile interaction problem with high computational efficiency, is adopted to obtain the mobilized soil-pile pressure above the slip surface and the subgrade reaction below the slip surface. Thereafter, an illustrative slope example is studied to explore the influence of soil spatial variability on the performance of stabilizing piles and failure modes of the reinforced slope.

### 2 Method

#### 2.1 SW model for spatially variable soil slope with stabilizing piles

Consider, for example, the stability analysis of a slope stabilized with a row of piles shown in Figure 1. The stabilizing piles are divided by the critical slip surface into a cantilever section and an embedded section. The

cantilever section is above the slip surface and subjected to a non-linearly distributed lateral driving force from the upper sliding mass. The embedded section is embedded below the slip surface and bearing the resistance from stable soil. Within the framework of the method of slice, the upper driving force (i.e.,  $F_{d-u}$ ), the upper resistance (i.e.,  $F_{r-u}$ ), the lower driving force (i.e.,  $F_{d-l}$ ) and the lower resistance (i.e.,  $F_{r-l}$ ) can be obtained by accumulating the forces of all slices. The lateral driving force ( $F_D$ ) transmitted to the pile from the upper slope can be evaluated as  $(F_{d-u}-F_{r-u}) \times S$ , where the  $S$  is the spacing of the piles. The iteration of SW model is then employed to calculate the soil-pile pressure until the total soil-pile pressure is equal to the  $F_D$ .

In SW model, the passive pressure area is simplified as wedge-shaped, and the mobilized soil-pile pressure is obtained based on the interaction between deformed piles and the sliding mass of the slope. Firstly, the initial strain above and below the slip surface are assumed to obtain the initial upper and lower strain wedges. The geometry parameter of the wedge in uniform soil is controlled by the fan angle  $\varphi_m$ , base angle  $\beta_m$ , the width of wedge  $BC$  and the diameter of the pile  $D$  (Figure 2(a)). For the spatially varied soil, multilayer is adopted to divide the soil into several sublayers with a uniform height of  $h$ . For the stabilizing pile, the  $i$  represents the given soil layer corresponding to the sublayer. Then, the spatial variability of soil properties are simulated by the Cholesky decomposition method with Gaussian autocorrelation function to generate the cross-correlated random variables (i.e., soil cohesion  $c$  and friction angle  $\varphi$ ), and the correlation of different sublayers is obtained based on the distance between the centroid of each sublayer. Afterwards, random field variables can be assigned to the corresponding sublayers to obtain a set of wedges with different geometries (Figure 2(b)). In order to obtain the geometry parameters of wedges,  $\varphi_m$  is governed by stress level in the soil and can be obtained from effective stress analysis (Ashour *et al.*, 1998), then the  $\beta_m$  and  $BC$  for each wedge can be derived as:

$$(BC)_i = D + (H_s - x_i) \cdot 2(\tan \beta_m)_i \cdot (\tan \varphi_m)_i \quad (1)$$

$$(\beta_m)_i = \frac{\pi}{4} + \frac{(\varphi_m)_i}{2} \quad (2)$$

where  $H_s$  is the sliding soil zone above the slip surface with a fixed depth and  $x_i$  is the depth from the top of the wedge to the centroid of the sublayer. Then, the soil-pile pressure  $p_D$  for each wedge in the cantilever section is obtained as follow:

$$(\Delta\sigma_{hf})_i = \left[ \left( \frac{C_i}{\tan(\varphi_i)} + (\bar{\sigma}_{v0})_i \right) \cdot \left[ \tan^2\left(\frac{\pi}{4} + \frac{\varphi_i}{2}\right) - 1 \right] \right] \quad (3)$$

$$(\Delta\sigma_h)_i = (SL)_i \cdot (\Delta\sigma_{hf})_i \quad (4)$$

$$\tau_i = (\bar{\sigma}_{v0})_i \cdot 2 \cdot (\tan \varphi_m)_i + 4 \cdot (C_m)_i \quad (5)$$

$$(p_D)_i = (\Delta\sigma_h)_i \cdot (BC)_i \cdot S_1 + 2 \cdot \tau_i \cdot D \cdot S_2 \quad (6)$$

where  $\bar{\sigma}_{v0}$  is the effective stress;  $SL$  is stress level which can be obtained from stress-strain model analysis by using the assumed strain mentioned above;  $C_m$  is the mobilized cohesion of soil which can be obtained from effective stress analysis (Ashour & Ardalan, 2012);  $S_1$  and  $S_2$  are the shape factors of piles that are 0.75 and 0.5, respectively, for circle piles, and both 1.0 for square piles. Then, the total soil-pile pressure  $P_D$  is equal to the sum of the soil-pile pressure of each sublayer (i.e.,  $P_D = \sum(p_D)_i$ ).

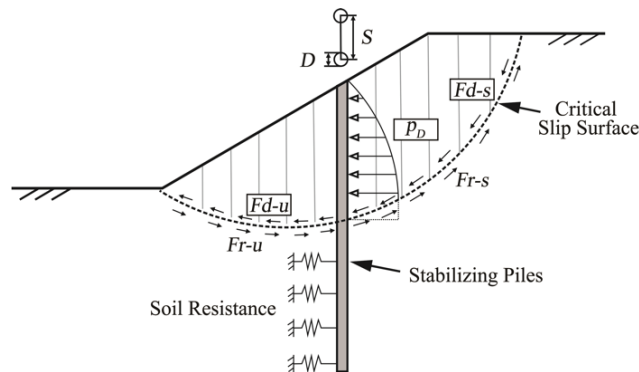
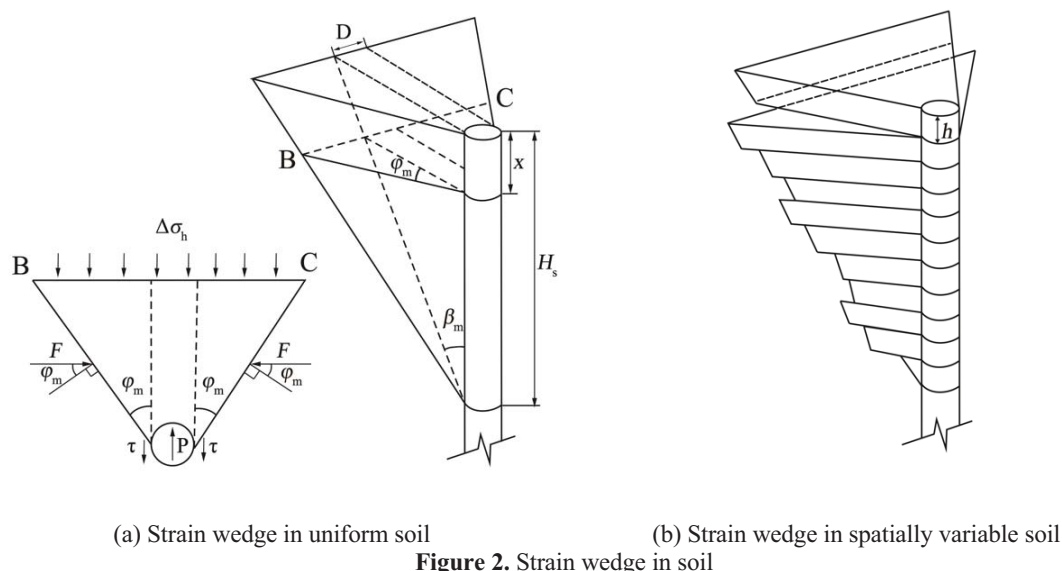


Figure 1. Schematic figure of the slope stabilized with piles.

After the analysis of the upper wedge, the SW model is adopted again to analyse lower wedges to obtain the modulus of subgrade reaction profile ( $E_s$ ) for the part of soil below the slip surfaces (Ashour *et al.*, 2004). To account for soil-pile interaction, the analysis of stabilizing pile is modeled as a beam with different segments of load in the cantilever section (i.e.,  $p_D$ ) and resistance of nonlinear elastic supports in the embedded section. The three-dimensional soil-pile interaction is simplified to the one-dimensional beam on elastic foundation (BEF) problem. Then, the BEF problem can be solved by using the finite element method and the pile response (e.g., bending moment, shear force, and deflection) can be obtained. By generally increasing and adjusting the strain in the upper and lower wedge, the soil-pile pressure would gradually increase. Finally, the iteration stops when the total soil-pile pressure ( $P_D$ ) reaches the lateral driving force from the upper slope (i.e.,  $P_D = F_p$ ) which refers to the state of soil-pile equilibrium. As a result, the deflected piles bear the residual driving force from the upper sliding mass and interact with surrounding soils with the balance between the driving force and soil resistance.

To concisely illustrate the procedure of the analysis of the slope-pile system, the steps are summarized as follows: (1) Characterizing the slope geometry and determine the parameters of soils and stabilizing piles; (2) Simulating the spatial soil variability by using the random field theory and incorporating the random field variables with sublayers; (3) Conducting slope stability analysis by Morgenstern–Price method and extracting the driving force and resistance of each slice from the stability analysis result and summing the driving force and resistance in the upper part of slope and lower part of slope to obtain the residual driving force from the upper part of the slope; (4) Using the SW model to obtain the  $P_D$  upon slip surface and  $E_s$  below the slip surface and determine the pile-head deflection  $(Y_0)_{SWM}$ ; (5) Solving the BEF problem to obtain the pile-head deflection  $(Y_0)_{BEF}$ ; (6) By adjusting the strain above and below slip surface, the result can be obtained when  $(Y_0)_{SWM} = (Y_0)_{BEF}$ ; (7) By generally increasing the strain of the wedge, the iteration ends when the failure occurs or the soil-pile pressure is equal to the driving force from the reinforced part of slope. The detailed failure criterion will be illustrated in the next section.



Regarding the analysis of slope with spatial variability, Monte-Carlo Simulation (MCS) shows simplicity and robust capabilities to deliver probabilistic analysis. To this end, the MCS is adopted to investigate the probabilistic characteristic of pile-reinforced slope in this study. The analysis of slope is repeatedly performed a large number of times with different random field variables to characterize the statistical characteristic of the result of slope stability and piles performance.

## 2.2 Failure modes of the pile-reinforced slope

In the analysis of SW model for pile-reinforced slope, different failure mechanisms can be accounted for the slope and piles. Three typical types of failure modes are adopted to cease the increase of load from the slope and to obtain the final performance of the pile. Failure mode I refers to the structural failure of stabilizing piles when the bending moment of the pile exceeds its ultimate value and the pile turned into plastic failure. Failure mode II is the soil failure when the  $SL$  in the wedge, which ranges between 0 and 1.0, exceeds 1.0. Failure mode III is the soil failure due to the group pile effect (Ashour & Ardalan, 2012). Along with the increase of load, the width of the wedge would increase and lead to the overlapping of the wedge of adjacent piles, and the soil in the overlapping area would fail when the  $SL$  exceeds 1.0.

### 3 Illustrative example

A cohesive-frictional soil slope laid on a bed rock modified from Ashour and Ardanan (2012) is used to study the effect of soil spatial variability on the response of pile and failure modes of the slope. The geometry of the slope is depicted in Figure 3. The statistics of the soil and rock properties are listed in Table 1. With the mean value of soil properties, the FS of the slope is calculated as 1.03 by using the Morgenstern–Price method with the half-sine function, and the corresponding critical slip surface is shown in Figure 3. As suggested by Ashour *et al.* (2004), the sublayer height is suggested for the range of 0.3 to 0.6 m. To this end, the sublayer height in element discretion is set as 0.5 m to consider soil spatial variability for the SW analysis. Typical realizations of the cross-correlated random fields of the cohesion and friction angle are shown in Figure 4. The diameter, length, spacing and elastic modulus of the circle piles are 1.2 m, 20 m, 3 m and  $2.6 \times 10^7$  kPa, respectively. For the structural failure criterion of the pile, the limiting bending moment (i.e., pile turned into elastic deformation) is 5000 kN/m.

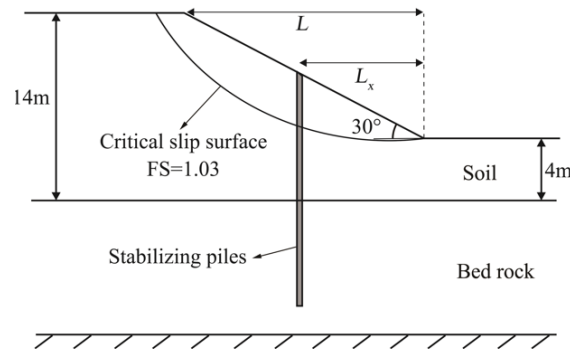


Figure 3. Slope geometry

Table 1. Statistics of soil and rock properties for the slope.

Type	$c$ (kPa)	$\varphi$ ( $^\circ$ )	$\gamma$ (kN/m $^3$ )	Distribution	Correlation length	Cross-correlation
Soil	Mean: 7.5 COV: 0.2	Mean: 17 COV: 0.2	19	Lognormal	4 m	$\rho_{c,\varphi} = -0.5$
Bed rock	700	30	20	-	-	-

Note: COV means coefficient of variation.

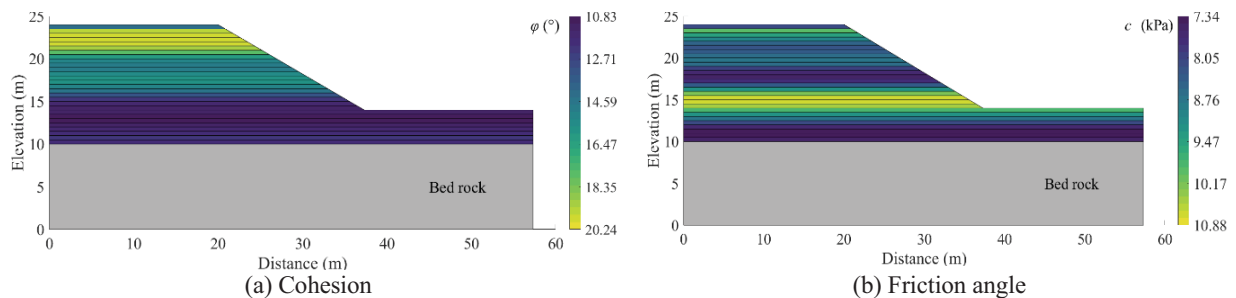


Figure 4. Typical realizations of random fields

#### 3.2 Influence of the spatial soil variability on the pile response

This section investigates the soil spatial variability on the responses of piles. By virtue of MCS, three characteristics, such as the bending moment, shear force and deflection, are used to represent the status of the pile under the lateral force from the reinforced slope part (i.e.,  $F_D$ ). Typical realizations of pile response with 100 MCS samples are presented in Figure 5. The pile responses based on the mean values of soil parameters are plotted by the red dashed line while the pile responses based on spatially variable parameters are represented by the grey line. It can be observed in Figure 5 (a) that the bending moment of the pile in spatially variable soil shows significant variations, indicating that the traditional deterministic analysis would be biased. As shown in Figures 5 (b) and (c), the distribution of the shear force and deflection shows a similar pattern to the bending moment. This observation indicates that the spatial variability can lead to the variation of the responses of piles under the lateral loading and soil resistance. The reason is probably that the soil spatial variability can lead to different shapes of the strain wedges as well as different driving forces from the upper slope and resistances in the stable section. The difference of lateral forces and the subgrade reaction provide the BEF analysis for the piles and then lead to the variation of response. Besides, it is observed in Figures 5 (a) and (b) that the maximum

bending moment and shear force for different random field realizations lie in different depths. This reason can be attributed to the spatial variability of soil properties that could result in different critical slip surfaces. Different locations of slip surfaces may lead to different embedded pile lengths in stable soil and then result in the different depths of the peak for different random field realizations.

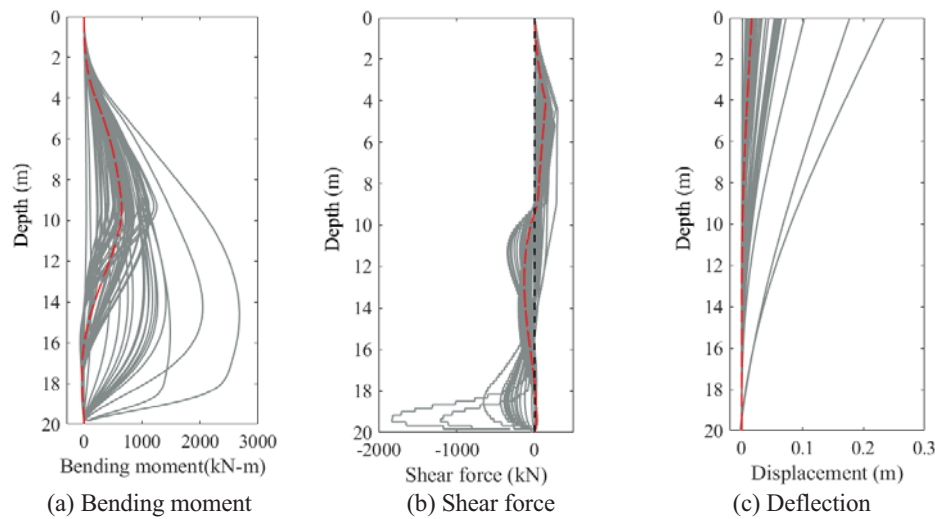


Figure 5. Pile responses under soil spatial variability

### 3.2 Influence of the soil spatial variability on failure mode

This section investigates the influence of the soil spatial variability on the failure modes of the slope-pile system. For pile-reinforced slope with a relatively high factor of safety, the driving force from the slope may not lead to failure of the system. Hence, the soil strain induced by the movement of the upper slope is made to increase gradually until the soil or pile fail. As shown in Figure 6, a sensitive study is firstly adopted to determine the MCS sample size. It can be observed that the percentages of three failure modes vary considerably when the number of MCS samples is less than 100 and gradually converge after 150. To keep a balance between computation efficiency and accuracy, the number of MCS samples is determined as 200 in the following analyses.

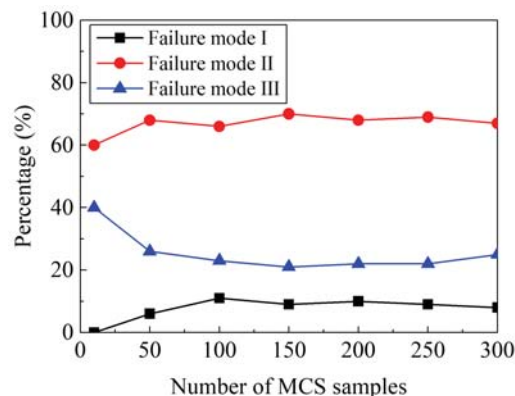


Figure 6. Number of MCS samples versus percentage of failure modes

Subsequently, the effect of different values of correlation length and coefficient of variation (COV) on the failure modes of the pile-reinforced slope was analyzed. With the mean values of soil properties, the slope failed with Failure mode II. When considering soil spatial variability, the slope exhibits multiple failure modes. In Figure 7 (a), it can be observed that the percentage of failure mode I increases first with the increase of the correlation length and then keeps stable at around 10%. The percentage of failure mode III decreases as the correlation length increases while the percentage of failure mode II increases as the correlation length increases. This result indicates that when correlation length decreases, the soil failure caused by the group pile effect is the dominated failure mode in the pile-reinforced slope.

As for the COV of the soil properties, a higher COV would result in a larger uncertainty within the soil properties (i.e., higher standard deviation). It can be observed in Figure 7 (b) that the percentage of failure modes I increases as the increase of the COV, and the percentage of failure modes II decreases as the COV increases. The percentage of failure modes III increases first with the increase of the correlation length and then decreases when the correlation length is larger than 0.3. When the COV decreases, the failure mode II becomes the



dominant failure mode for the reinforced slope. Besides, it can be observed that with the increase of the correlation length and decrease of COV, the percentage of failure modes II gradually increase. This is expected because a larger correlation length and smaller COV indicates more homogeneous soil and the result is closer to the slope failure with the mean values of soil properties.

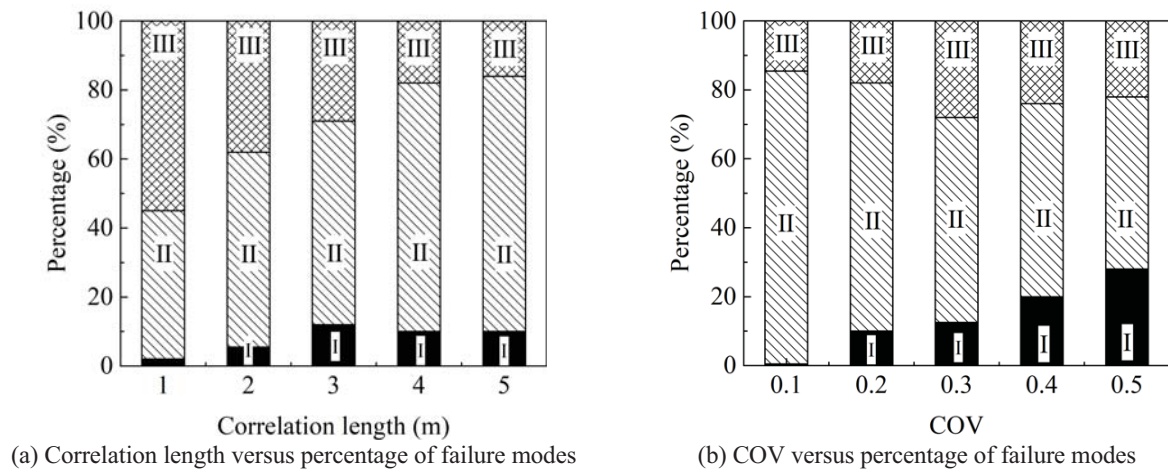


Figure 7. Influence of correlation length and COV of soil properties on failure modes

#### 4 Summary and Conclusions

This paper investigates the spatial variability of soil properties on pile responses and failure modes of pile-reinforced slope considering soil-pile interaction. The results show that the spatial variability of soil properties has a significant influence on the responses of the piles and failure mechanisms. Compared with homogeneous soil, stabilizing piles in spatially variable soils show significant variations in bending moment, shear force and deflection. The conventional determined analysis method may lead to biased results of failure modes of pile-reinforced slope and failure modes. Besides, a higher heterogeneity and uncertainty of soil variability could lead to a higher possibility of structural failure of piles and the group effect failure.

#### Acknowledgements

The work described in this paper was funded by grants from the National Natural Science Foundation of China (Project No. 41902291), the Natural Science Foundation of Hunan Province, China (Project No. 2020JJ5704), the Open Research Fund Program of Key Laboratory of Metallogenic Prediction of Nonferrous Metals and Geological Environment Monitoring (Central South University), Ministry of Education (Project No. 2020YSJS21), the Fundamental Research Funds for Central South University (Project No. 2021zzts0268), the Science and technology innovation leading project of high-tech industry of Hunan Province, China (2020GK2067), and China Scholarship Council (CSC No.202106370134). The financial support is greatly acknowledged.

#### References

- Ashour, M. & Ardalan, H. (2012). Analysis of pile stabilized slopes based on soil–pile interaction. *Computers and Geotechnics* 39, 85-97.
- Ashour, M., Norris, G. & Pilling, P. (1998). Lateral Loading of a Pile in Layered Soil Using the Strain Wedge Model. *Journal of Geotechnical and Geoenvironmental Engineering* 124, 303-315.
- Ashour, M., Pilling, P. & Norris, G. (2004). Lateral Behavior of Pile Groups in Layered Soils. *Journal of Geotechnical and Geoenvironmental Engineering* 130, 580-592.
- Gong, W., Tang, H., Wang, H., Wang, X. & Juang, C. H. (2019). Probabilistic analysis and design of stabilizing piles in slope considering stratigraphic uncertainty. *Engineering Geology* 259, 105162.
- Jiang, S. H., Huang, J. S., Huang, F. M., Yang, J. H., Yao, C. & Zhou, C. B. (2018). Modelling of spatial variability of soil undrained shear strength by conditional random fields for slope reliability analysis. *Applied Mathematical Modelling* 63, 374-389.
- Kontoe, S., Summersgill, F., Potts, D. & Lee, Y. (2022). On the effectiveness of slope stabilising piles for soils with distinct strain-softening behaviour. *Geotechnique* 72, 309-321.